https://doi.org/10.5194/tc-2022-232
Preprint. Discussion started: 5 December 2022

The Cryosphere Discussions

A field study on ice melting and breakup in a boreal lake, Pääjärvi, in Finland

Yaodan Zhang[1,2], Marta Fregona[3], John Loehr[2], Joonatan Ala-Könni[4], Shuang Song[5,6], and Matti Leppäranta[2], and Zhijun Li[1]

[1]State Key Laboratory of Coastal and Offshore Engineering, Dalian University of Technology, Dalian, China
[2]Lammi Biological Station, University of Helsinki, Finland
[3]Department of Civil, Environmental and Mechanical Engineering, University of Trento, Italy
[4]Institute of Atmospheric and Earth Sciences, University of Helsinki, Helsinki, Finland
[5]Water Conservancy and Civil Engineering College, Inner-Mongolia Agricultural University, Hohhot, China
[6]College of Water Conservancy, Shenyang Agricultural University, Shenyang, China

Correspondence to: Zhijun Li (lizhijun@dlut.edu.cn), Yaodan Zhang (zhangyaodan@mail.dlut.edu.cn).

Abstract. Lake ice melting and breakup form a fast, nonlinear process with important mechanical, chemical, and biological consequences. The process is difficult to study in the field due to safety issues, and therefore relatively little is known about its details. In the present work, ice monitoring was based on foot, hydrocopter, and boat to get a full time-series of the evolution of ice structure and geochemical properties through the melting period. The field observations were made in Lake Pääjärvi during the ice decay periods in 2018 and 2022. In 2022, the maximum thickness of ice was 55 cm with 60 % snow-ice, and based on the data and heat budget analysis, the ice melted by 33 cm from the surface and 22 cm from the bottom while porosity increased to 40–50 % at breakup. In 2018, the snow-ice layer was small and bottom and internal melting dominated during the decay. Due to global warming, the ice breakup date became earlier. The mean melting rates were 1.31 cm d^{-1} in 2022 and 1.55 cm d^{-1} in 2018. In 2022 the electrical conductivity (EC) in ice was 11.4±5.79 S cm^{-1}, one order of magnitude lower than in the lake water, and ice pH was 6.44±0.28, lower by 0.4 than in water. pH and EC of ice and lake water decreased along the ice decay except slight increases in ice due to flushing by lake water. Chlorophyll *a* was less than 0.5 g L^{-1} in porous ice, approximately one-third of that in the lake water. These results are important for further development of numerical models and understanding the process of ice decay with consequences to lake ecology and to safety of ice cover for human activities.

1 Introduction

Lake ice is a thin layer between the atmosphere and lake water and plays an important role in the meteorological, hydrological, biological, geochemical and socio-economical regimes of boreal lakes (Leppäranta, 2015). Lake ice affects the local weather altering the heat, mass and momentum exchange between the atmosphere and water bodies and increase the albedo, reducing the solar radiation transfer into the water (Ellis and Johnson, 2004; Rouse et al., 2008a, 2008b; Williams et al., 2004). The physical properties of ice cover are determined by stratification, crystal structure, gas bubbles and porosity. These properties to a large degree control ice mechanics, acoustics, optics, thermodynamics and electrodynamics which have a key role in ice remote sensing, the living conditions under-ice, and the ecology within ice (Iliescu and Baker, 2007; Li et al. 2010; Shoshany et al., 2002). Although most boreal lakes possess a seasonal ice cover, lake research has traditionally focused on summer, and especially little is known about the decay of ice when the ice starts to melt and weaken. The obvious reason is that at this time fieldwork is logistically very difficult to carry out. However, the physical and geochemical properties of ice undergo rapid changes during the ice decay period that has an important influence on conditons on and below the ice cover.

There are two major practical problems with melting lake ice due to loss of ice strength caused by the deterioration of ice (Ashton, 1985; Leppäranta, 2015; Masterson, 2009). The bearing capacity of ice decreases, and therefore on-ice traffic becomes risky. Accidents are reported every spring due to ice breakage, connected with fishing or crossing of lakes. The variations of ice structure during the ice decay period seriously impact the form and time of ice breakup in the spring. Decreasing ice strength implies that ice cover may be broken by wind and drift on shore. Also, moving ice with finite strength is a risk for hydraulic structure, such as lake site platforms, bridges and a force for near-shore erosion. Hence, it is urgent to study the physical properties of ice during melting period.

The climatology of ice breakup date has been widely studied based on long-term time-series records (Benson et al., 2012; Korhonen, 2006; Karetnikov et al., 2017; Magnuson et al., 2000). A steady trend toward earlier melting date has been reported in most recent ice phenology studies, by about one week over 100 years and can be attributed to the global climate warming. Some numerical modelling studies of ice breakup date revealed that the time when ice starts to melt and the internal deterioration has

https://doi.org/10.5194/tc-2022-232
Preprint. Discussion started: 5 December 2022

important impact on the accuracy of simulations (Yang et al, 2012). The physics of climate sensitivity and the relationship to the timing of ice breakup is a question of atmospheric warming and falling albedo (Leppäranta, 2014). Understanding better this phenological change requires a quantification of the physical mechanisms that control the melting of ice.

The trend for earlier melting of lake ice is considered to be the driving factor for the changes of ecological and biogeochemical processes in seasonal ice-covered lakes (Garcia et al, 2019; Griffiths et al, 2017). Lake ice interacts with under ice water to further drive or facilitate the migration and transformation of nutrients and metals, resulting in changes in the biomass and structure of phytoplankton (Cavaliere and Baulch, 2018; Schroth et al, 2015). In addition, the habitat conditions and ecosystem structure under the ice affect the limnology of the following seasons (Hampton et al., 2017). pH, Electrical conductivity (EC) and Chlorophyll *a* (Chl *a*) are important indicators of ecological environment and have significant impacts on the primary productive. However, it is uncommon to see pH, EC and Chl *a* quantified during ice decay period. In general, an overall lack of knowledge of the extent to how ice melting affects ecological and biogechemical process limits the properly assess the impacts of climate change on limnological process in cold regions (Tan et al., 2018).

In the period of ice cover decay, the snow layer melts first. Due to its low light transmissivity, the snow cover protects the ice by its presence (Ashton, 1986; Leppäranta, 2015; Warren, 1982). Also, the high albedo of snow delays the start of the ice decay period. The situation changes immediately when the snow melting begins, and the snow cover disintegrates. Then ice melting begins, and also sunlight penetrates the ice to heat the water under the ice depending on the spring weather and ice quality (Kirillin et al. 2012). At the same time, primary production begins and as the ice melts, all impurities contained in the ice are released into the water or to the air which may change the water environment. Normally primary production peaks after ice breakup; thus, ice melting is connected to the spring bloom. Due to the difficult conditions with unstable and deteriorating ice cover, there has not been much in situ research during the ice melting period. Knowledge of melt rate is limited to a few studies, with typically 1−3cm d^{-1} in terms of equivalent ice thickness, seen at the top and bottom boundaries and in the ice interior, depending on the weather conditions (Jakkila et al., 2009; Leppäranta et al., 2010, 2019; Wang et al., 2005; Yang et al., 2012). Surface melting is mainly related to the albedo. It was found that the

https://doi.org/10.5194/tc-2022-232
Preprint. Discussion started: 5 December 2022

transmittance changed with the internal melting and the amount of gas pockets and water-filled pockets in ice (Jakkila et al., 2009). Internal melting opens channels for flushing the ice by surface melt water and lake water. It is mainly reflected in the increase of porosity. When the porosity of ice has reached the level of around 0.5, ice cover collapses by its own weight and then disappears rapidly (Leppäranta et al., 2010, 2019). Bottom melting is caused by the heat flux from water that can be large in spring, and in the cold season this heat flux provides a limitation for the ice growth (Shirasawa et al., 2006; Yang et al., 2012).

We examine here the decay of ice cover in Lake Pääjärvi, southern Finland by field surveys and ice and water samples in two years, April 2018 and 2022. This lake is frozen for 4–5 months annually, and the ice cover consists of congelation ice and snow-ice with snow cover on top (Jakkila et al., 2009; Wang et al., 2005). The decay of ice cover takes about one month, and the process is controlled by the presence of snow on top and the optical quality of snow, in addition to atmospheric and solar forcing. The structure and properties of the ice are changing during the decay process, and the actual melting of the ice takes place at the surface and bottom and in the interior. This paper gives the final results of the field campaigns.

2 Materials and methods

2.1 Study site

Lake Pääjärvi is located in the boreal zone in southern Finland (61°40′ N, 25°08′ E). The lake area is 13.4 km^2, the mean and maximum depths are 14.4 m and 87 m, respectively, and the catchment area is 244 km^2 (Arvola et al., 1996). Lake Pääjärvi is a humic, brown-water lake with an average optical depth of 0.67 m and Secchi depth of 1.8 m (Arst et al., 2008). The ice season lasts normally 4–5 months. In the period 1910–1988, the mean freezing and breakup dates were December 13 and May 5, respectively. For the breakup date the standard deviation was 8 days, the earliest and latest dates were April 14 and May 18, respectively, and the maximum annual ice thickness was 50 cm with standard deviation of 9 cm (Kärkäs, 2000). The fraction of snow ice was on average one-third in 1993–1999 (Leppäranta and Kosloff, 2000).

https://doi.org/10.5194/tc-2022-232
Preprint. Discussion started: 5 December 2022

The field study was made in Pappilanlahti Bay in the west side of the lake. This bay is shallow (maximum depth <15 m), with three small inflows at the end of the bay and a weak groundwater flux at the bottom. There was access to the lake ice from a platform at the shore by foot and in late season by a hydrocopter and a boat. Our field observations were made as a pilot study in 12−20 April 2018 and as the main experiment in 25 March−3 May 2022, of which the latter case was more extensive and thus provides the body of the data. The ice situation was recorded by ground and drone orthophotos and field notes, and ice and water samples were collected several times. In 2022 the whole decay period was mapped while in 2018 just the last eight days of it.

2.2 Observations

In the pilot study in 2018, the field site was visited five times between April 12 and April 20. The study was focused on a short period at the end of ice decay. On April 12, 15 and 20 ice samples were taken. After April 20, because of the rapid melting, it was not possible to walk on the ice or to use a boat for sampling, but photographs were taken daily from the shore. Otherwise sampling work was done in similar manner as in 2022.

In 2022 the monitoring took 40 days on a weekly basis. Each time the ice quality and thickness were checked first. Ice samples (whose lateral cross-section was 30 cm × 30 cm) were cut by drill and saw and stored then in a freezer. Water samples were taken from the drill holes and analysed in the laboratory for pH, EC and Chl *a*. The ice samples were analysed in a cold room (–10 °C) for the crystal structure and density. Ice melt water was also analysed for the pH, EC and Chl *a* the same way as the water samples.

The study period in 2022 covered the whole decay process. Eight field site visits were made from March 25 to May 3. The sampling was made by foot from shore until April 22. Since April 26, melting begins from the shoreline and there was a slush layer between the surface ice and the congelation ice layer, the bearing capacity of the ice was not strong enough for walking on the ice at the latest phase of the melting period. Then, a hydrocopter was used for ice sampling on April 26–29 (Fig. 1a). On May 3, the melting created several open channels, a boat was used for ice sampling. The freeboard, snow

https://doi.org/10.5194/tc-2022-232
Preprint. Discussion started: 5 December 2022

The Cryosphere Discussions

thickness, snow-ice thickness, and congelation ice thickness were measured by ruler during the ice sampling and the water samples were collected after the ice sampling into a sealed bottle.

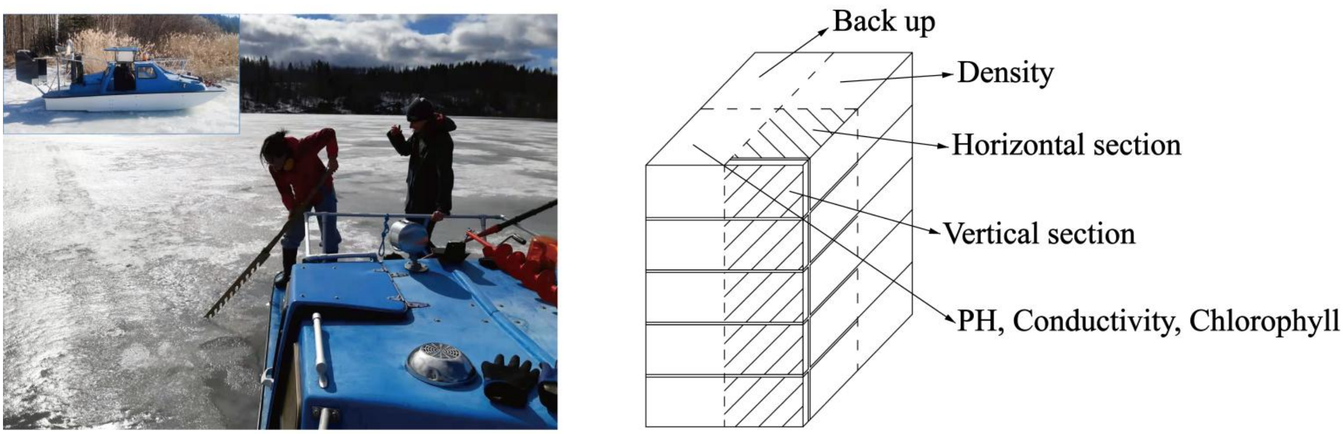

(a) (b)

Figure 1. Lake ice sampling and processing: (a) collect ice with a handsaw on the hydrocopter; (b) the ice block was sliced into four parts for different observations.

All ice and water samples were put into plastic bags at the site and transported immediately to Lammi Biological Station (about 500 m away from the site). Then, the ice samples were stored in a freezer at a temperature of −18 °C, and the water samples were stored in fridge at a temperature of 4–6 °C. In the analysis, each ice sample was divided into four sections. Section 1 was cut vertically into layers, and then the pH, EC and Chl *a* of the layers was measured from the meltwater. Section 2 was cut vertically and horizontally to map the ice crystal structure and study the gas bubbles by image analysis, Section 3 was used to measure the density of ice, and Section 4 was stored as a backup (Fig. 1b).

Available routine meteorological and hydrological data of the Finnish Meteorological Institute (FMI) and Finnish Environment Institute (SYKE) were utilized. SYKE data include manual measurements of thicknesses of ice, snow-ice and snow, and freeboard every ten days during the whole winter in Pappilanlahti Bay, and FMI provided the meterological data of an automated station in the yard of the Lammi Biological Station half a kilometre from our site. The SYKE data was used for the all-season ice and snow thickness, while the melting period data were own field observations. The data base of the Lammi Biological Station was utilized for the long-term ice phenology and geochemistry of inflows from brooks into the study bay.

https://doi.org/10.5194/tc-2022-232
Preprint. Discussion started: 5 December 2022

2.3 Laboratory work

The ice crystal structure, gas bubbles, and ice density were studied from the ice samples in the INAR (Institute of Atmospheric and Earth Sciences, University of Helsinki) ice laboratory. The crystal structure was obtained from thin sections. The samples were cut into vertical sections of 8–10 cm height by a bandsaw, and horizontal sections were extracted at the vertical cuts. The sections were frozen on glass plates to be prepared for thin sections. The size and distribution of gas bubbles in the ice were observed under normal light, and ice crystal structure was obtained from thin sections between crossed polarizers (Deng et al., 2019; Langway, 1958).

Measurements of ice density can be found in several studies (Timco and Frederking, 1996). The mass/volume method was used to measure the ice density in laboratory, and the freeboard in the field was used as a control. In the laboratory, the sample was cut into 5 cm cuboids by a bandsaw. The sides of a cuboid were measured by vernier caliper, and the mass was measured by an electronic scale with the accuracy of 0.001 g.

For the geochemistry, the samples were cut into vertical sections based on the structure at an interval of 8–10 cm by a bandsaw. Then, the blocks were melted in sealed bags, the water was poured into sample bottles and stored in a fridge (at 4–6°C). pH and EC were measured from unifiltered samples according to the standard in SFS-EN 27888 and SFS 3021. By using a Thermo Orion 3-STAR Precision Benchtop pH meter and YSI 3200 conductivity sensor, respectively. These two instruments offer high accuracy for water analyses and multipoint calibration. The amount of the Chl *a* was measured from filtered sub-samples by Shimatzu UV-1800 spectrophotometer (Arvola et al. 2014). The absorbance of Chl *a* was extracted at a long wavelength.

3 Results

3.1 Ice structure

The ice decay period began on March 25 and the final breakup took place on May 5, 2022 (Table 1). The thickness of ice was 55 cm on March 25. The ice was melting at both boundaries and in the interior. On April 22, it was still possible to walk on ice when the total thickness was 38 cm but the ice was quite

https://doi.org/10.5194/tc-2022-232
Preprint. Discussion started: 5 December 2022

The Cryosphere Discussions
Open Access
EGU

porous. The decay period was 42 days. The melting rate increased toward the end, and the mean value was 1.31 cm d^{-1}.

Table 1. Thickness of ice layers and freeboard in the melting phase (cm) and porosity (%) in 2022, also shown is the ratio of freeboard to draft.

2022	Snow-ice	Congelation ice	Total ice	Porosity	Freeboard	Fb/draft	Snow
March 25	33	22	55	x	5.5	0.11	1
April 1	31	20	51	6.1	5	0.11	2.5
April 8	30	17	47	x	2	0.044	13
April 14	31	17	48	7.7	5	0.12	2
April 22	27	11	38	15.2	4	0.12	0
April 26	7.5 + 7¶	10	24.5	17.1	1	0.0057	0
April 29	6 + 12¶	4	22	24.1	0.5	0.0023	0
May 3	z	2–z	2	34.0	x	x	0
May 5	z	2–z	0	0	0	x	0

¶ Surface ice + slush layer

Generally, when deterioration is occurring the ice cover has a grayish, splotchy appearance from above and appears treacherous (Ashton, 1985). Figure 2 shows images of the ice cover recorded by drone orthphotos at an altitude of 100 m during the melting period. The snow fell at the beginning of April turned the ice white. As the air temperature rose, the snow on the ice began to melt, creating a patchy surface that deteriorated until the ice broke up.

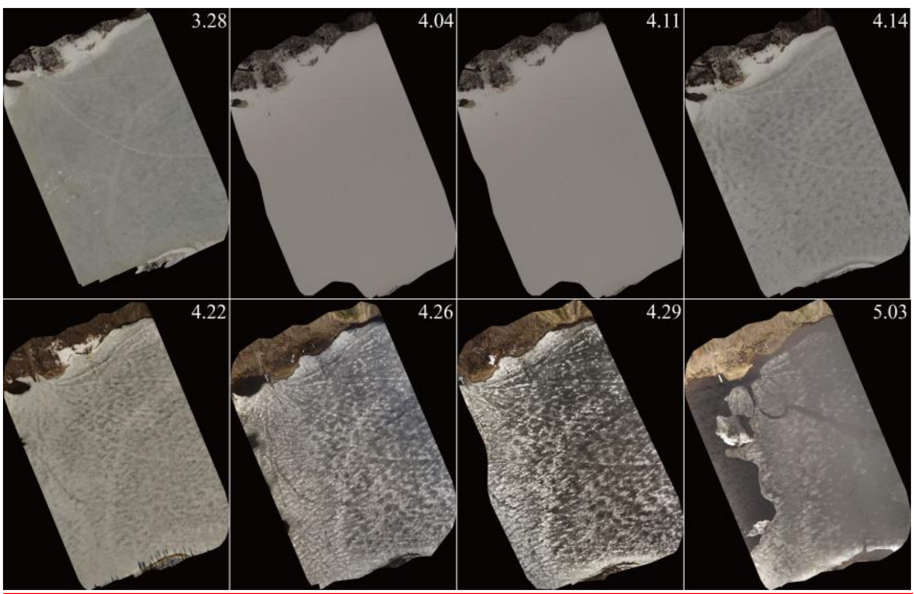

Figure 2. Drone orthophotos of the ice cover in the melting period (time given as month.day).

https://doi.org/10.5194/tc-2022-232
Preprint. Discussion started: 5 December 2022

The melting period began in late March. The maximum annual ice thickness of 55 cm was well within the range of long-term statistics where the mean value is close to half meter (Kärkäs, 2000). As we can see from Fig. 3a–f, there were two principle vertical layers in the Lake Pääjärvi ice cover. The top layer was granular snow-ice, the grain size was 1–9 mm with blurred crystal boundaries, and the lower layer was columnar congelation ice. The columnar ice layer was clear ice with the grain size of 2–10 cm. With the increasing air temperature, the ice crystal structure results showed that the thickness of both snow-ice and congelation ice decreased, and the porosity became more and more.

The ice melted 4 cm in May 25–April 1 (0.57 cm d^{-1}). On April 1, it was seen from the crystal structure that the shape of snow-ice crystals above 28 cm was very irregular with blurred crystal boundaries, and the grain size was mainly within 1–2 mm. The grain size of the 28–32 cm layer was mainly within 2–5 mm, granular crystals with clear boundaries. It can be judged that the top 0–28 cm layer was snow-ice that had undergone the thawing-refreezing process, and the 28–32 cm layer was the surface congelation ice layer formed at the beginning of the ice season. The columnar ice layer underneath was clear ice with grain size increasing with depth, range from 2 to 10 cm. There was a volume of 4–6 % rachis shaped and spherical shaped gas bubbles in snow-ice with the maximum diameter of 4 mm, and a volume of 1–2 % spherical shaped gas bubbles in congelation ice with the maximum diameter of 1 mm. From the vertical sections, there was also a distinct boundary between granular ice and columnar ice at around 32 cm.

Then, in April 1–14 the melting was 4 cm (0.30 cm d^{-1}), but the thickness of snow-ice was unchanged. According to the weather data, continuous snowfall began on April 5, and the temperature rose after that, resulting in the formation of new snow-ice through the melt-freeze cycle. Compared with April 1, the ice crystal size had not changed, but the temperature rose from April 10 to 14. The bubble content in the snow-ice was 5–7 %.

After April 14, the temperature continued to rise, and the ice rapidly melted, 10 cm in April 14–22 (1.25 cm d^{-1}). The horizontal and vertical sections showed that severe melting occurred at the snow-ice grain boundaries. The gas content in snow-ice increased to 6–10 % and 1–3 % in congelation ice. Also, the maximum diameter of gas bubbles increased to 5 mm in snow-ice and 3 mm in congelation ice.

https://doi.org/10.5194/tc-2022-232
Preprint. Discussion started: 5 December 2022

In April 26–29 (0.83 cm d^{-1}), a slush layer appeared below a surface ice layer due internal melting of ice. Since April 26, the columnar ice began to melt at crystal boundaries, and gas inclusions appeared at the boundaries. On April 29, gas bubbles also appeared in the inside columnar crystals, with the bubble content reaching 5 % and the maximum bubble size reaching 5 mm. On May 3, the columnar ice and slush layers had melted, and 2 cm snow-ice left.

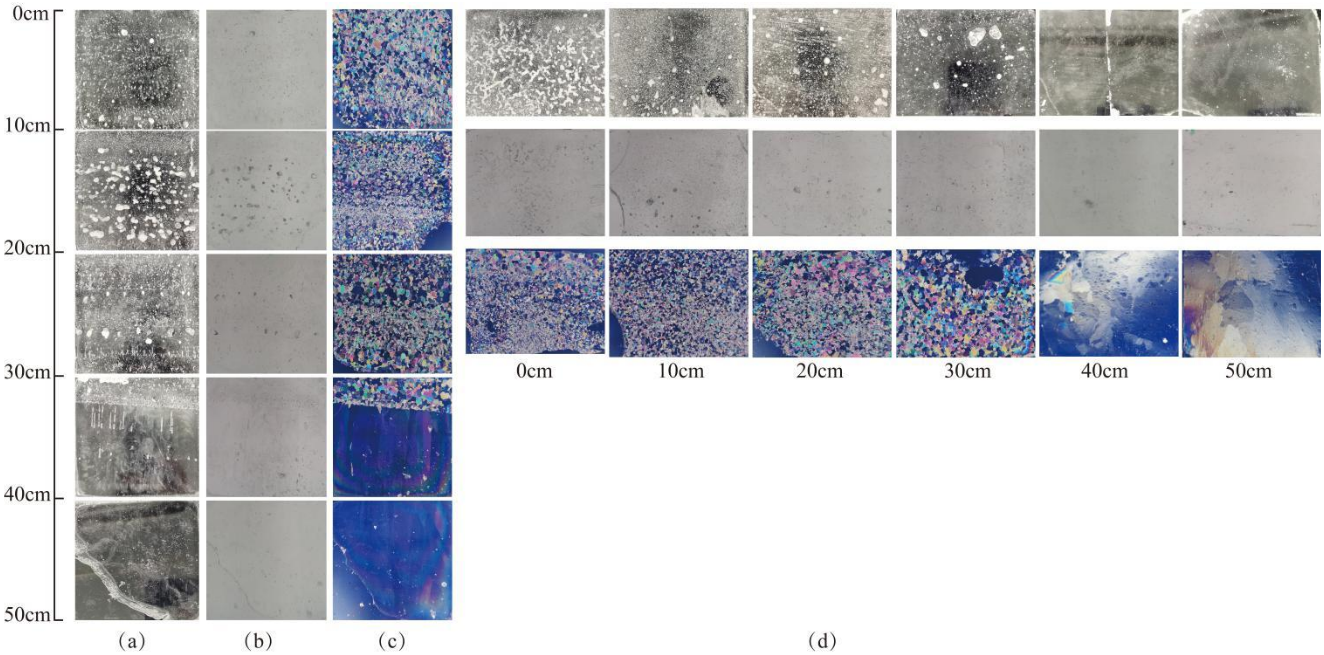

Figure 3a. Lake Pääjärvi ice crystal structure of April 1.

https://doi.org/10.5194/tc-2022-232
Preprint. Discussion started: 5 December 2022

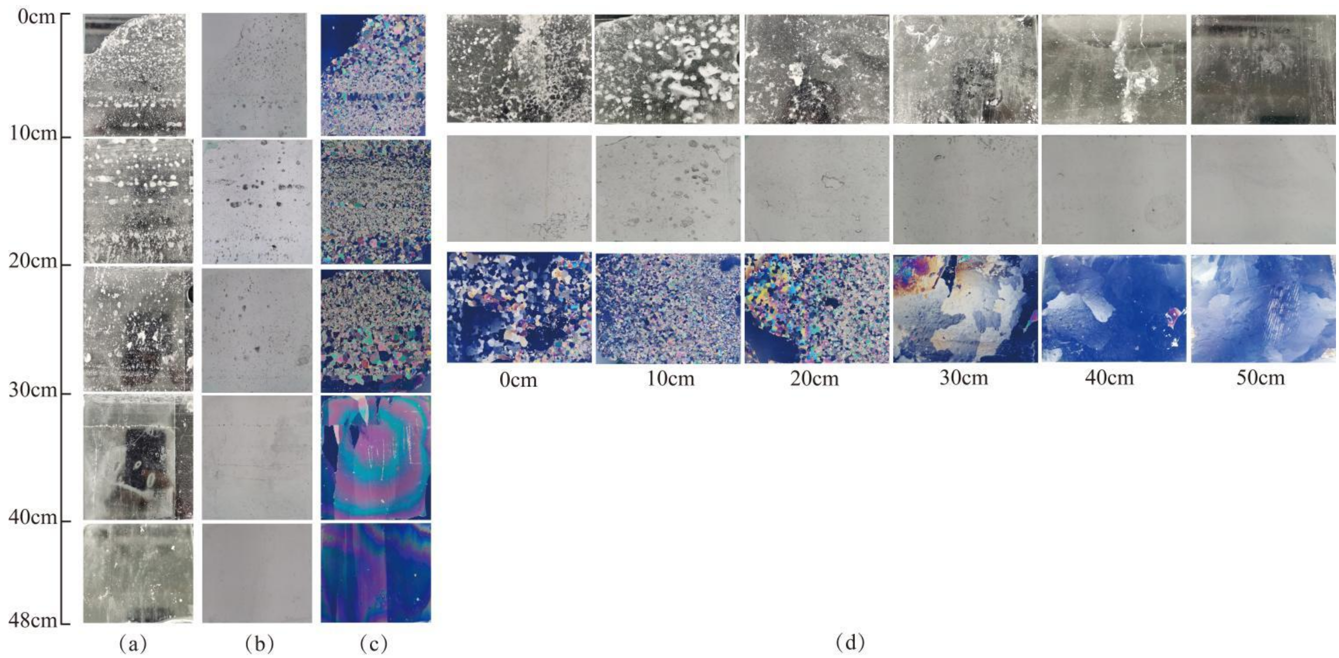

Figure 3b. Lake Pääjärvi ice crystal structure of April 14.

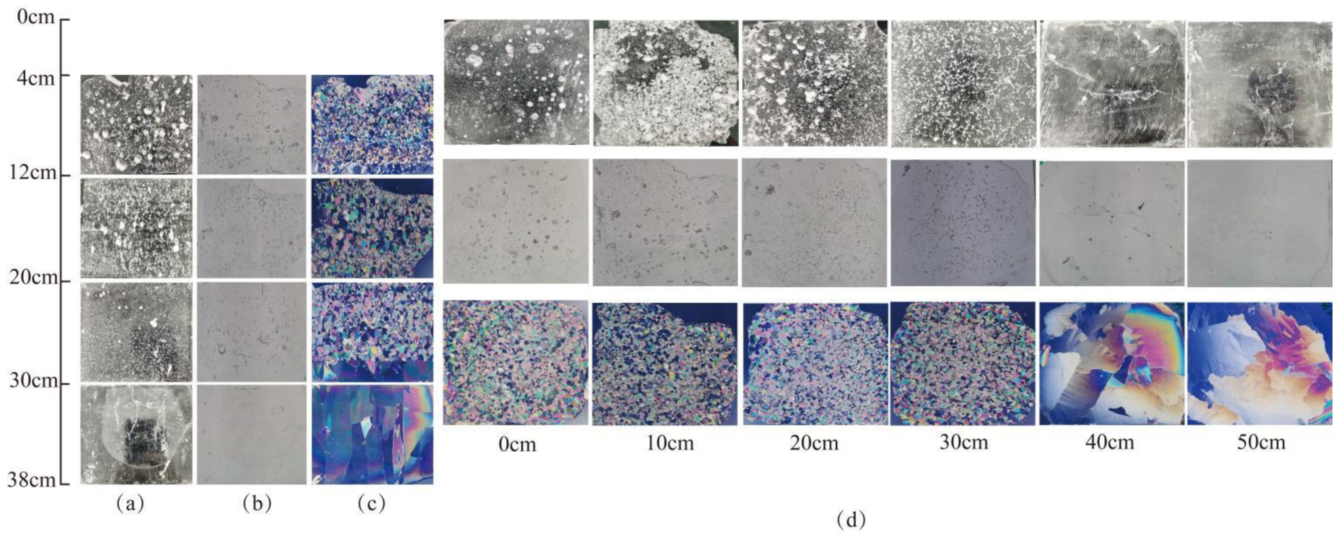

Figure 3c. Lake Pääjärvi ice crystal structure of April 22.

https://doi.org/10.5194/tc-2022-232
Preprint. Discussion started: 5 December 2022

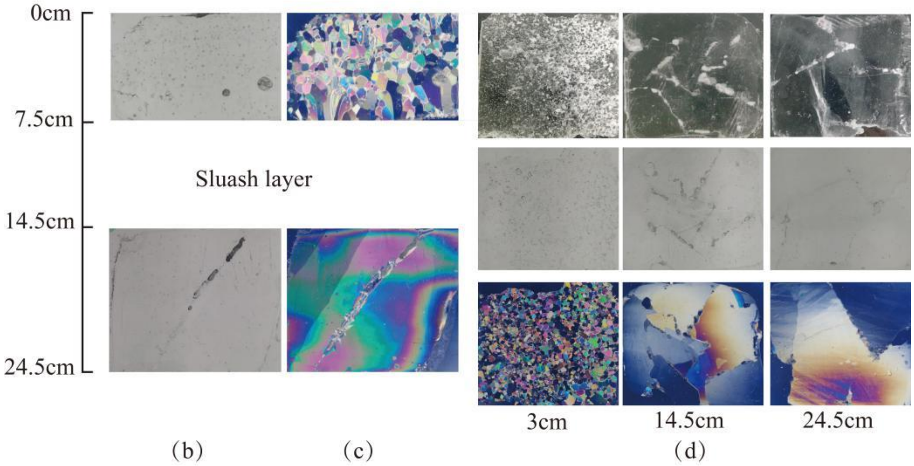

Figure 3d. Lake Pääjärvi ice crystal structure of April 26.

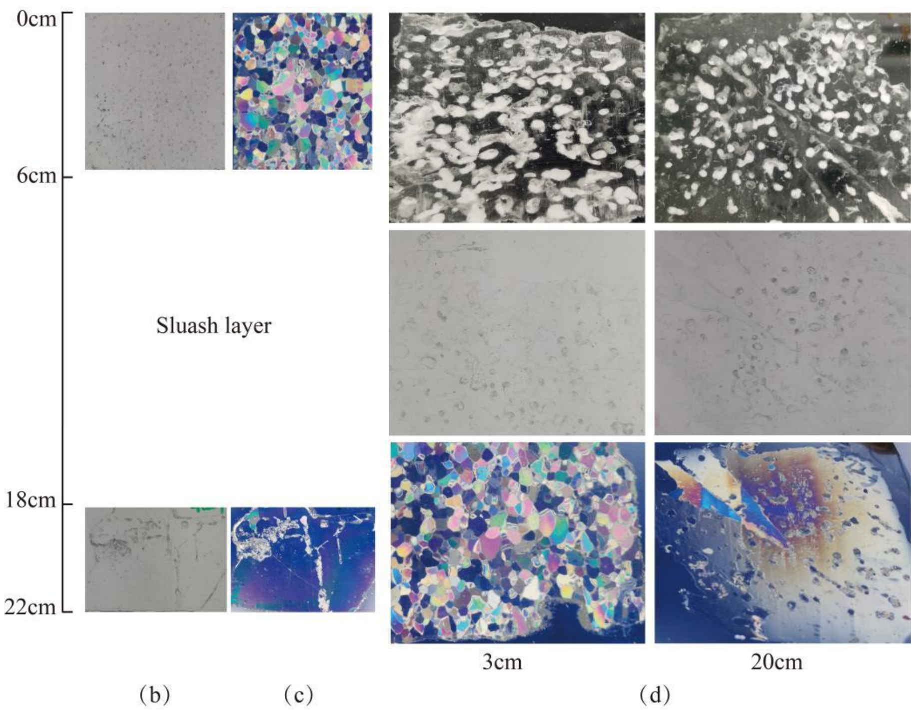

Figure 3e. Lake Pääjärvi ice crystal structure of April 29.

https://doi.org/10.5194/tc-2022-232
Preprint. Discussion started: 5 December 2022

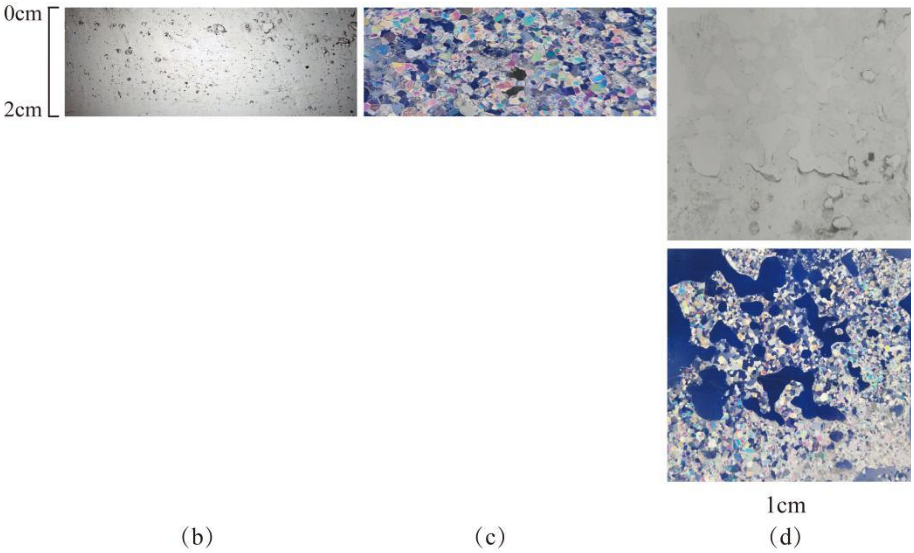

Figure 3f. Lake Pääjärvi ice crystal structure of May 3.

Figure 3. Lake Pääjärvi ice crystal structure between March 25 and May 3.(a) photographs of gas bubbles with the thickness of the vertical cross-section around 5mm in normal light; (b) photographs of gas bubbles with the thickness of the vertical cross-section around 1mm in normal light; (c) photographs of the vertical cross-section of the crystal structure in polarized light; (d) photographs of the horizontal cross-section of gas bubbles and crystal structure. Photographs of gas bubbles with the thickness of the vertical cross-section around 5mm in normal light were missing on April 26, April 29 and May 3.

In 2018, the decay period also began at the end of March, and the final breakup took place on April 25. The thickness of ice was 42 cm on March 30. The ice was melting by 0.5 cm d^{-1} at the bottom, and on April 2 a 14 cm new snow layer fell and then melted in 10 days. On April 12 the ice was bare and solid, and ice thickness was 35.0 cm, consisting of 5.3 cm snow-ice and 29.7 cm congelation ice. In April 5–10, the average daily air temperature was above 0 °C, but in April 10–15 it was below 0 °C in the night time. It was raining on April 1, 3, 8, 19, and on the 24th the rain greatly accelerated the melting. After April 12, the thickness of ice started to decrease along with the rising air temperature and solar radiation (Table 2). The ice melted 4 cm in April 12–15, in April 15–20 the melting was 12.7 cm, and by April 20 the 5.3 cm snow-ice layer had melted fully while congelation ice thickness had decreased by 9.4 cm with 20.3 cm remaining. Between 12–20 April, it was possible to walk on the ice from the shore. In all, the ice decay period lasted 27 days, and the mean melt rate was 1.55 cm d^{-1}.

Table 2. Thickness of ice layers and freeboard in the melting phase (cm) and porosity (%) in April 2018, also shown is the ratio of freeboard to draft.

https://doi.org/10.5194/tc-2022-232
Preprint. Discussion started: 5 December 2022

2018	Snow-ice	Congelation ice	Total ice	Porosity	Freeboard	Fb/draft
April 12	5.3	29.7	35.0	~ 0	3.0	0.094
April 13	4.7	29.3	34.0	x	3.0	0.097
April 14	3.3	28.7	32.0	x	2.0	0.067
April 15	2.7	28.3	31.0	x	2.0	0.069
April 20	0	20.3	20.3	25	x	x
April 25	0	0	0	x	0	x

The ice sample data in Tables 1–2 were used to determine the melting at the surface (snow-ice) and bottom (congelation ice), and the porosity was used to estimate internal melting. The result for 2022 (Table 3) shows that the snow-ice melted from the top and congelation ice from the bottom almost fully, and the last 2 cm piece was snow-ice. The mean melt rate at the bottom was 0.38 cm d^{-1} in March 25 – April 26 that corresponds to the energy flux of

$$\frac{h_f}{h_d} = \frac{\rho_w - \rho_d}{\rho_f} = 13 \text{ W m}^{-2}, \qquad (1)$$

where ρ_i is ice density, L_f is the latent heat of freezing and the time is $\Delta t = 1$ d. The energy flux was a little larger than normally assumed. The internal melt rate was 0.18 cm d^{-1} equivalent thickness that was limited due to the low transmittance of snow-ice. In the last week of existence the structure of ice was highly porous and internal breakages occurred.

Table 3. Ice melting in spring 2022 (cm). The numbers show the change from the row above to the present one.

2022	Surface melt	Bottom melt	Total melt	Internal melt
March 25	0	0	0	0
April 1	2	2	4	x
April 8	1	3	4	0.4
April 14	-1	0	-1	0.4
April 22	4	6	10	3.2
April 26	4.5	1	5.5	0.6
April 29	4.5	6	10.5	1.6
May 3	16	4	20	1.2
May 5	2	0	2	0
Sum	33	22	55	7.4

Winter 2018 ice cover was different from 2022 in that the ice was mostly (85 %) congelation ice. Table 4 shows that the snow-ice had all melted by April 20 when there was still 20.3 cm congelation ice left. In 12–20 April the surface melting was 5.3 cm, the bottom melting was 9.4 cm, and internal melting

https://doi.org/10.5194/tc-2022-232
Preprint. Discussion started: 5 December 2022

was 6.9 cm. The ice was more transparent that allowed more sunlight penetration through ice than in 2022. The bottom melting in 12–15 April corresponds to the heat flux of 16 W m^{-2} from water to ice.

Table 4. Ice melting in spring 2018 (cm). The numbers show the change from the row above to the present one.

2018	Surface melt	Bottom melt	Total melt	Internal melt
April 12	0	0	0	0
April 13	0.6	0.4	1.0	x
April 14	1.4	0.6	2.0	x
April 15	0.6	0.4	1.0	x
April 20	2.7	8.0	10.7	6.9
April 25	z	20.3–z	20.3	x

3.2 Ice density

At the initial stage of melting, in April 1–14, 2022, the average densities of snow-ice and congelation ice were 850 kg m^{-3} and 970 kg m^{-3}, respectively. Since April 22, no new snow-ice was formed and the ice continued melting at the surface, bottom and in the interior. Accordingly, the ice density profiles were moved along the direction of ice depth, as shown in Fig. 4, and the depth of the movement was consistent with the ice melting thickness from the surface. In the melting process, the density of snow-ice and congelation ice decreased gradually, with density higher with depth. In particular, on April 22 the snow-ice density increased greatly with depth. The pore channels in the ice did not penetrate into water, and internal melting may have caused meltwater to accumulate in some parts of the ice, resulting in large ice density, even more than the density of ice on April 14. The average density of snow-ice was 730 kg m^{-3} and the average density of congelation ice was 930 kg m^{-3} on April 22. Finally, from April 26 to May 3, the average density of snow-ice and congelation decreased to 690 kg m^{-3} and 770 kg m^{-3}, respectively. The density data were used to estimate the porosity, which was found to increase from 6.1 % to 34 % during the melting season (Table 1).

https://doi.org/10.5194/tc-2022-232
Preprint. Discussion started: 5 December 2022

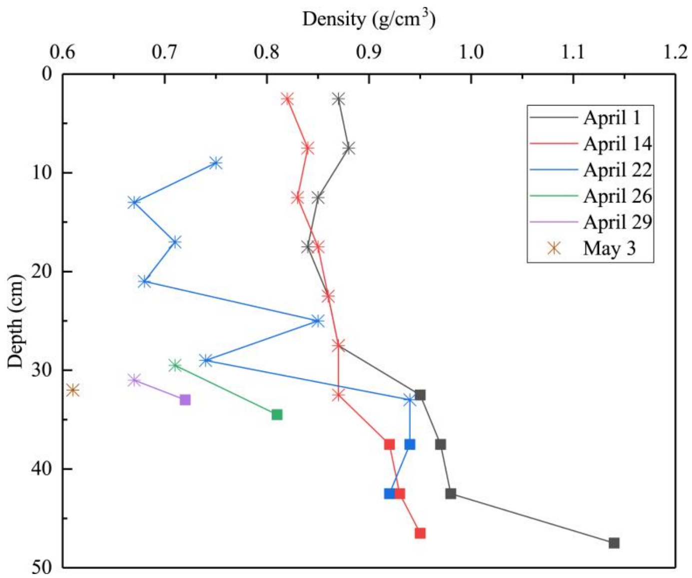

Figure 4. Lake Pääjärvi ice density profiles (asterisk stands for snow ice, cube for congelation ice).

For bare ice, the freeboard/draft ratio is

$$\frac{h_f}{h_d} = \frac{\rho_w - \rho_d}{\rho_f}, \qquad (2)$$

where h is total ice thickness, ρ is density, and the subscripts are for water, d for draft, and f for freeboard. In winter, for $\rho_f = \rho_d \approx 910$ kg m^{-3}, this ratio is 0.099 or $^{1}/_{10}$. It increases when the porosity decreases, but it may decrease if meltwater drainage from freeboard is trapped inside the draft to reduce the buoyancy. This is consistent with field observation in 2022 and 2018. In practice it is difficult to determine the freeboard/draft ratio as it requires an order of one-millimetre accuracy for the freeboard.

3.3 Ice geochemistry

During the melting period, meltwater was mixed into the surface layer below the ice and influenced the water chemistry. The meltwater had lower pH and EC than the lake water (Table 5), and consequently lower density (Kirillin et al., 2012), and therefore a thin fresh surface layer could form just under the ice. In the winter of 2021–2022, before the snowfall on April 5, the pH and EC of snow-ice decreased. The mean pH of snow-ice was 6.47 on March 25 and 6.38 on April 1, and in these dates the mean EC were 23.0 S cm^{-1} and 17.3 S cm^{-1}, respectively. Then EC decreased with average value of 9.34 S cm^{-1} on April 14 still slightly decreasing thereafter. In congelation ice, EC was consistently within 8–11 S cm^{-1}.

https://doi.org/10.5194/tc-2022-232
Preprint. Discussion started: 5 December 2022

With the process of ice decay, melting in upper layer of the ice cover drained down into the lower layer of the ice cover which caused the higher EC of April 1 20–31 cm, April 8 30–40 cm and April 14 42–48 cm. Until April 22, pH was smaller in in snow-ice than in congelation ice but EC were greater in snow-ice than in congelation ice. After the slush layer was created on April 26, pH, EC and Chl *a* were slightly higher in the bottom congelation ice than in snow-ice due to the flooding of the lake water. The chlorophyll *a* content was greater in snow-ice than in congelation ice but less than that in lake water before April 22.

In the winter of 2017–2018, EC was stable at 97 S cm^{-1} under ice until dropping to 81 S cm^{-1} on April 20th. pH beneath the ice also decreased slightly in the progress of melting, from 6.87 to 6.77. In ice meltwater, EC was 6 S cm^{-1} and pH was 6.35.

Table 5. pH, EC and Chl *a* in ice meltwater and water under ice at the study site in 2022 and 2018.

Year	Date	Depth (cm)	Ice type	Ice			Under ice		
				pH	EC (μS cm^{-1})	Chl *a* (μg L^{-1})	pH	EC (μS cm^{-1})	Chl *a* (μg L^{-1})
		0–10	Snow-ice	6.47	31.1	0.3			
		10–20	Snow-ice	6.46	24.3	0.3			
	March 25	20–30	Snow-ice	6.46	13.6	0.6	x	x	x
		30–40	Cong.ice	6.75	8.95	0.4			
		40–50	Cong.ice	6.75	8.94	< 0.1			
		0–10	Snow-ice	6.39	16.8	0.2			
		10–20	Snow-ice	6.38	14.0	0.2			
	April 1	20–31	Snow-ice	6.36	21.3	0.6	x	x	x
		31–40	Cong.ice	6.69	8.54	< 0.1			
		40–50	Cong.ice	6.69	8.53	0.1			
		0–10	Snow-ice	6.35	9.66	0.2			
2022		10–20	Snow-ice	6.35	8.17	0.5			
	April 8	20–30	Snow-ice	6.34	10.7	0.6	x	x	x
		30–40	Mix-ice	6.62	16.3	0.2			
		40–50	Cong.ice	6.64	8.51	0.3			
		0–11	Snow-ice	6.28	10.8	0.4			
		11–22	Snow-ice	6.28	8.92	0.3			
	April 14	22–34	Snow-ice	6.29	8.56	0.3	6.81	102.9	0.2
		34–42	Mix-ice	6.60	8.51	0.2			
		42–48	Cong.ice	6.56	9.92	0.1			
		0–14	Snow-ice	6.25	7.53	0.3			
	April 22	14-28	Snow-ice	6.25	7.31	0.3	6.79	92.2	0.2
		28–38	Cong.ice	6.51	6.93	0.2			

https://doi.org/10.5194/tc-2022-232
Preprint. Discussion started: 5 December 2022

	April 26	0–7.5	Snow-ice	6.24	7.53	0.5	6.74	84.9	0.6
		14.5–24.5	Cong.ice	6.58	7.71	0.4			
	April 29	0–6	Snow-ice	6.25	7.60	0.5	6.79	74.1	1.7
		18–22	Cong.ice	6.58	8.72	0.4			
	May 3	0–2	Snow.ice	6.47	10.3	0.5	6.98	81.2	1.7
	April 12						6.86	97	
	April 13						6.87	97	
2018	April 14			6.39	6		6.83	97	
	April 15						6.81	97	
	April 18			6.30	6		6.80	96	
	April 20						6.77	81	

The mean ± standard deviation of pH, EC in the ice were 6.44 ± 0.28 and 11.4 ± 5.77 S cm^{-1} in the winter 2021–2022. In lake water, the corresponding quantities were 6.82±0.09 and 92.5±12.7 S cm^{-1}. The mean value of EC in snow-ice and congelation ice were of the same order of magnitude but by one order of magnitude lower than that in the lake water, in exact form EC(ice) = 0.12·EC(water). The same result was found in the winter of 2018–2019. The mean value of pH in snow-ice was 6.34, a little lower than 6.63 in congelation ice. The deposition of acidic substances from the atmosphere was the background for the low pH of snow-ice. This can also be confirmed by the data of EC on April 14. EC of ice decreased with the ice melting, but increased after the snowfall on April 5. The mean value of Chl *a* content in ice was less than 0.5 g L^{-1}, 0.35 times of that in lake water.

Figure 5 shows pH, EC and Chl *a* in snow-ice, congelation ice and lake water with the ice melting process. The mean pH and EC in ice and lake water decreased with ice decay. However, they slightly increased after the slush layer appeared on April 26. The main reason is that after the slush layer appeared, some lake water flooded into the slush layer, and the high pH and EC in lake water caused their slight increase in the ice. EC was lower in congelation ice than in snow-ice at the beginning of ice decay, and after April 8 they became very close because of melting effects. Chl *a* was very low since the ice limited the transmission of light, and photosynthesis in ice and water was very weak. But as the thickness of the ice decreased, the transmission of light increased, primary production continued to rise and the content of Chl *a* in the ice and water increased gradually. Algae can grow in a slush layer within snow-ice, but not in consolidated ice because of lack of liquid water for living organisms. The present article reported that the Chl *a* in snow-ice is greater than in congelation ice but less than in water.

https://doi.org/10.5194/tc-2022-232
Preprint. Discussion started: 5 December 2022

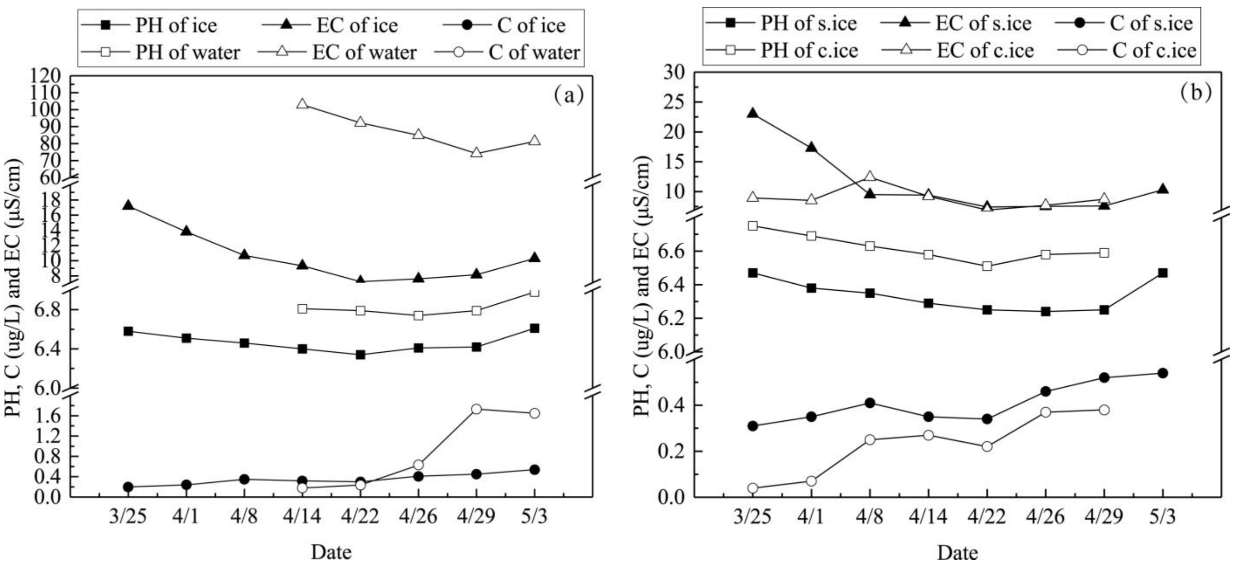

Figure 5. The mean pH, EC and Chl *a* in ice and lake water in 2022 (left) and the mean pH, EC and Chl *a* in snow-ice (s.ice) and congelation ice (c.ice) (right).

4 Heat budget

The heat content of lake ice was used to analyze the observations of ice melting. The heat fluxes include solar radiation, terrestrial radiation, turbulent air-ice fluxes at the surface, precipitation, and heat flux from the water body to ice bottom (e.g., Leppäranta, 2015). In the melting period, we consider the volume of ice per unit area (V), expressed by the ice thickness (h) and porosity (ν) as $V = (1 - \nu)h$. It is assumed that in the melting stage the ice is isothermal with the temperature at the melting point. The mass balance is then given by (Leppäranta et al., 2019)

$$\rho_i L_f \frac{dV}{dt} = -\left(Q_0 + Q_A + Q_w\right), \tag{3a}$$

$$\rho_i L_f (1 - \nu) \frac{dh}{dt} = -\left(Q_0 + Q_w\right), \tag{3b}$$

$$\rho_i L_f h \frac{d\nu}{dt} = Q_A , \tag{3c}$$

Where ρ_i is ice density, L_f is latent heat of freezing, Q_0 is surface heat balance, Q_w is heat flux from water, and Q_A is absorption of solar radiation in ice. At $\nu = \nu^* \sim 1/2$, ice breaks due to its own weight and the remains melt then fast.

In the melting period, the surface heat budget is dominated by the radiation balance with solar radiation having a key role (Wang et al., 2005: Jakkila et al., 2009). The input fluxes in Eq. (3b) can be estimated by (see Leppäranta, 2015)

$$Q_0 = k_0^{'}(t) + k_1(T_a - T_0), \quad (4)$$

where $k_0^{'}$ depends on solar radiation and therefore on time, and k_1 ~15 W m^{-2} °C^{-1}. It is assumed that $k_0^{'}$ takes half of the solar radiation while the other half is let to penetrate the near-surface layer. Then we obtain a representative, climatological $k_0^{'}$ by interpolation from the mean values of –48 W m^{-2} in March, –34 W m^{-2} in April and 4 W m^{-2} in May based on Leppäranta (2015). The total modelled surface melting became 25 cm that is rather close to the result (33 cm) obtained from the ice structure analysis (Table 3). The value of $k_1 \sim 15$ W m^{-2} °C^{-1} corresponds to the degree-day coefficient of 0.43 cm (°C·d)$^{-1}$, which is close to the usual degree-day coefficient in hydrological forecasting (Leppäranta, 2015).

The question is then internal melting and bottom melting which depend on the solar radiation. We have (see Leppäranta et al., 2019)

$$Q_A = (1-\alpha)\gamma\left(1 - e^{-\lambda h}\right)Q_{s0}, \quad (5)$$

$$Q_w = Q_{w0} + c(1-\alpha)\gamma e^{-\lambda h} Q_{s0}\,, \quad (6)$$

where α is albedo, γ represent the fraction of light in solar radiation, and λ is the light attenuation coefficient. The climatological value of solar radiation in April is $Q_{s0} = 150$ W m^{-2}. Taking the optical parameters as $\alpha = 0.5, \gamma = 0.5, \lambda = 1$ m^{-1}, as the representative solar flux in April, we have $Q_A = 11$ W m^{-2} corresponding to melt rate of 0.32 cm d^{-1}, more than 0.18 cm d^{-1} obtained from the ice structure data. To evaluate the heat flux from the water, we can take $c = 0.3$ (Leppäranta et al., 2019), and then $Q_w = Q_{w0} + 9.1$ W m^{-2}, and according to estimate of $Q_w = 13$ W m^{-2} in Section 3.1, we have $Q_{w0} =$ 3.9 W m^{-2} that may look a bit large but can be explained by the inflow from brooks into the bay.

Thus, the comparison between ice structure and heat balance gives satisfactory agreement in the view of large uncertainties in both data sets. The heat balance gave the triple (surface melting, internal melting, bottom melting) as (25 cm, 14 cm, 11 cm), while the observed result was (33 cm, 8 cm, 22 cm). There was not good boundary layer data for above or below ice, and the optical parameters are only roughly known. It is concluded that the field data and heat budget were consistent within the limits of accuracy of observations. This means that the heat budget can be used to assess the melting of the ice and further predict the breakup of the ice.

In April 2018, ice thickness was 35 cm on the 12th, and ice breakup took place on the 25th. The last five days are not known for the evolution of the ice cover, but in 12–20 the surface melting was 5.3 cm, bottom melting was 9.4 cm, and internal melting was 6.9 cm (Table 4). With the melting formula (4–6) and mean air temperature over 12 – 20 April of 5.7 °C, we have the surface melting 11 cm, bottom melting 5 cm, and internal melting 2 cm. Again, these numbers have large uncertainty due to data limitations, but it is seen that there is certain consistency between ice structure and heat budget data.

5 Discussion

5.1 Ice season and interannual variations of ice breakup date

Ice phenology time-series includes ice freezing days and the ice freezing and breakup dates. Climate change studies based on ice phenology have been conducted for many lakes. Field observed ice data are very important for many single and multiple variable regression analyses used to develop regression models and physical models to predict the ice phenology (George, 2007; Williams et al., 2004; Stefen and Fang 1997). In the ice season 2021–2022, the air temperature fell below the freezing point of water at mid-November (Fig. 6) and primary ice formed in the study lake at the end of December (Shumskii, 1956). Thereafter congelation ice grew steadily downward, and snow-ice formed on the top mostly due to flooding of the ice. The seasonal maximum thickness of 55 cm was reached in late March. The ice freezing days and the date of ice freezing are affected by parameters that determine heat storage and release of the water body. In contrast, the ice breakup date depends on solar radiation and the characteristics of the ice and snow. The snow cover strengthened the albedo and blocked the exchange of heat between the atmosphere and ice that reduced congelation ice growth rate as well as prevented deterioration of the ice under snow. In the middle of March, the daytime air temperature started to be above the freezing point and snow melted first and disappeared by the end of March. Then, ice melting started, paused for a week due to snowfall on April 5 with a thin new snow-ice layer on ice. After mid-April ice melted by 2–3 cm d^{-1} and finally disappeared on May 5. The entire ice season lasted 149 days and the decay period was 42 days.

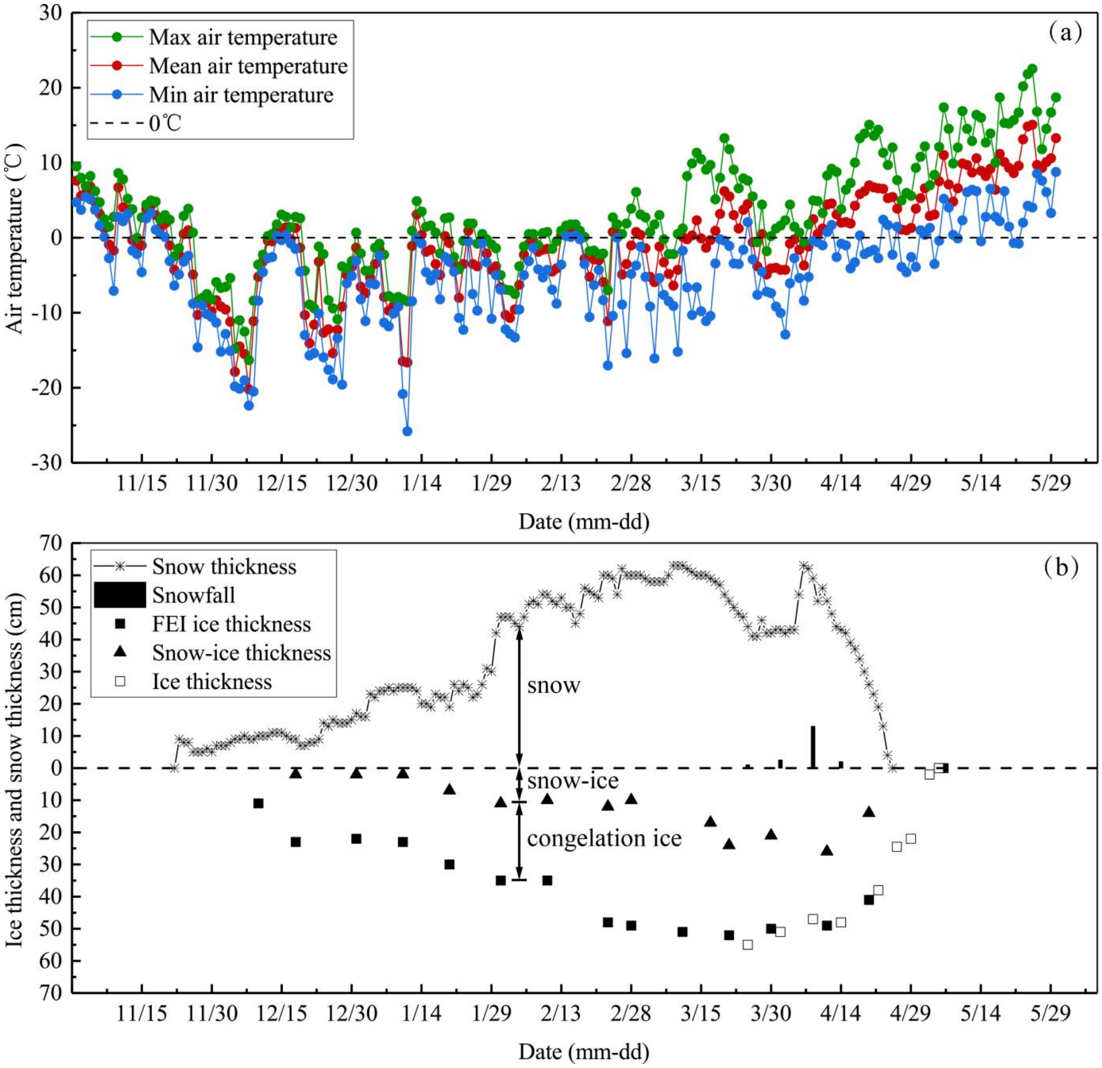

Figure 6. Air temperature and freezing data on Lake Pääjärvi during the winter of 2021-2022. (a) the max, mean and min daily air temperature from November 1 to May 30, (b) Snowfall in ice decay period, snow and ice thickness measured by Finnish Environment Institute (SYKE) from November 1 to May 6, and ice thickness measured by this research from March 25 to May 5.

https://doi.org/10.5194/tc-2022-232
Preprint. Discussion started: 5 December 2022

Climate variations have a major impact on ice season characteristics; in other words, ice season characteristics are sensitive indicators of climate. In the period from 1970 to 2022, the average length of ice season was 130 days in Lake Pääjärvi, and the standard deviation of 25 days showed a great dispersion. The ice breakup was on average April 25, with a standard deviation of 12 days. The time series is short but shows ice breakup becoming earlier in the last 50 years (Fig. 7). However, the interannual variability of the ice breakup date is quite high. In 1970–1990 the change was about 5 days per decade that is more than could be explained by global warming and the reason remains unclear. In general, in southern Finland the trend has been 0.5–1 days earlier breakup per decade. Results on the lake ice breakup date have shown change of only about 3–4 days per 50 years (Bernhardt et al., 2011; Magnuson et al, 2000). In an arctic tundra in Finland, Lake Kilpisjärvi, the trend from 1964 to 2008 was 2.2 days over 50 years towards earlier ice breakup (Lei et al., 2012). Reduced ice freezing days and earlier ice breakup could have a potentially widespread implications on 50 countries (Sharma et al., 2019). The loss of lake ice could lead to a reduction in the availability of fresh water due to increased rates of evaporation, as well as ice cultural and socio-economic impacts for lake ice recreation, such as ice fishing and skating.

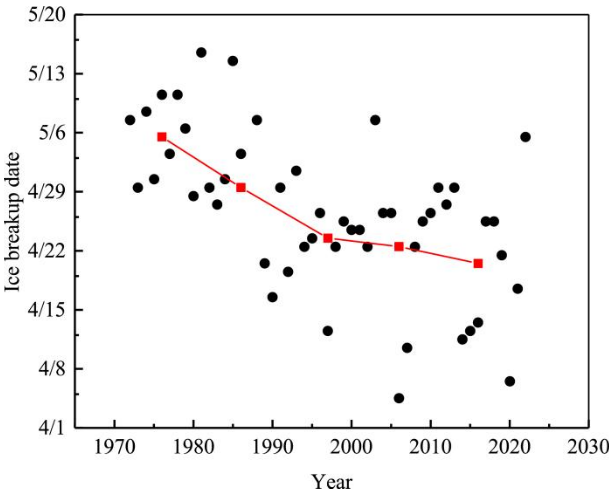

Figure 7. The ice breakup date of Lake Pääjärvi from 1970 to the present, the black dots indicate the ice breakup date while the res dots indicate the ice breakup date averaged in every 10 years. Data source: Lammi Biological Station.

https://doi.org/10.5194/tc-2022-232
Preprint. Discussion started: 5 December 2022

5.2 Comparisons with ice melting

Ice melting is related to air temperature, solar radiation, albedo, lake bathymetry and morphology, as well as the ice structure in particular on the fractions of clear congelation ice and opaque snow-ice. Melting begins after the net radiation becomes positive and takes place at the surface, interior and bottom depending on the surface heat fluxes and the absorption of solar radiation within the ice. Surface melting is not only reflected in a reduction in the thickness of ice but also in visible changes of the surface of the ice cover.

The melting of ice is illustrated by the accumulated melting thickness for the total and the surface, bottom, and internal portions separately (Fig. 7). In 2022, the surface melting was greater than the bottom melting, while in 2018, it was the opposite. The main reason was that the ice structure was different in these two ice years. In 2022, the snow-ice layer accounted for 60 % of the ice cover, while in 2018, the fraction was only 15 %. However, it can be seen from Fig. 7 that the melting of the surface layer and the bottom layer were increasing at the same time, and the melting rate was gradually increasing due to the weather was getting warmer and warmer and solar radiation increased continuously.

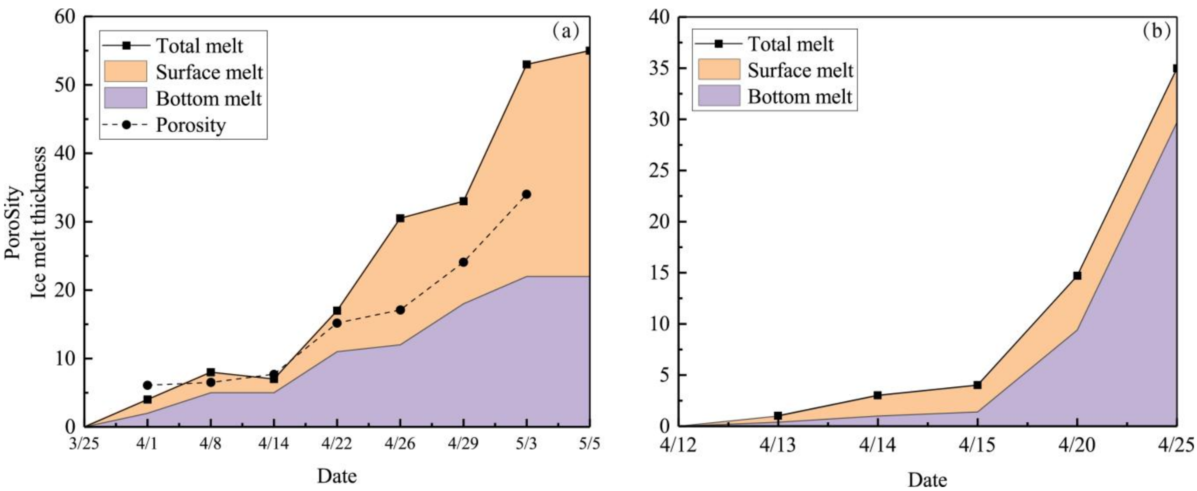

Figure 8. Accumulated ice melting and porosity in 2022 (left) and 2018 (right). Porosity was not recorded in 2018.

Overall, the mean ice melting rate was 1.31 cm d^{-1} in 2022. After the new snow had disappeared, the surface and bottom melt rates were 1.63 cm d^{-1} and 0.8 cm d^{-1}, respectively. In Lake Kilpisjärvi, Arctic tundra, the melting of ice had similar features with Lake Pääjärvi. In 2014 with normal weather

https://doi.org/10.5194/tc-2022-232
Preprint. Discussion started: 5 December 2022

conditions the rate was close to 2022 but larger in the very warm year 2013 (Leppäranta et al. 2019). In boreal lakes at 61 – 62 ° N, numerical modelling in Lake Vanajavesi (Yang et al. 2012) and field investigation in Lakes Vendyurskoe (Leppäranta et al. 2010) and Pääjärvi (Leppäranta et al. 2009) gave similar melting rates as here. The main results on ice melting, if further generalized, will provide the necessary quantitative information for estimating the seasonal response of ice to climate change.

https://doi.org/10.5194/tc-2022-232
Preprint. Discussion started: 5 December 2022

Table 6. ice data in other boreal lakes.

Lake	Date	Location	Average depth	Maximum depth	Ice season	Ice thickness	Ice melting rate
Vendyurskoe Leppäranta et al. (2010)	2006 2007	62°10′ N 33°10′ E	5.3 m	13.4 m	180–190 days Breakup date 10–20 May	60-69 cm	2006: 1.2 cm d^{-1} on the surface layer, 0.2 cm d^{-1} on the bottom layer; 2007: 1.2 cm d^{-1} on the surface layer, 0.8 cm d^{-1} on the bottom layer.
Kilpisjärvi Leppäranta et al. (2019)	2013 2014	69°03′ N 20°50′ E	19.5 m	57 m	4–6 months Breakup date in June	77–114 cm	2013: 2.9 cm d^{-1} on the surface surface, 1.0 cm d^{-1} in internal, 0.5 cm d^{-1} on the bottom layer; 2014: 0.8 cm d^{-1} on the surface, 1.0 cm d^{-1} in internal, 0.1 cm d^{-1} on the bottom layer; Mean melt rate: 1.3cm d^{-1}.
Pääjärvi Wang et al. (2005); Jakkila et al. (2009)	2004 2006	61°04′ N 25°08′ E	14.8 m	87 m	4–6 months	30–80 cm	1.25 cm d^{-1} on the surface layer.
Vanajavesi Yang et al. (2012)	2008	63°13′ N, 24°27′ E	7 m	24 m	4–6 months	45–60 cm	Mean melt rate: 1.3 cm d^{-1}

Ice thickness and temperature are the simulated ice properties in lake ice physical models (Ashton, 1986; Shirasawa et al., 2006; Leppäranta, 2009). This works during the ice growing season, but during the melting season, the variation of ice thickness does not tell of internal melting, for which porosity data are needed. Internal melting changes the structure of the ice, and once the porosity reaches around 50 %, the ice cannot bear its own weight, breaks, and disappears rapidly (Leppäranta et al. 2019). A study in

https://doi.org/10.5194/tc-2022-232
Preprint. Discussion started: 5 December 2022

Lake Pääjärvi in 2004–2006 found that the breakage resulted at the porosity of 45 % (Leppäranta et al. 2009). The present work measured ice density in the 2022 melting period, and the porosity corresponding to the measured ice density was used as the porosity estimator. The porosity increased with the ice melting (Fig. 7). The density of pure ice is 917 kg m^{-3} and the estimated porosity was 34 % on May 3, and the ice broke up on May 5 when the porosity of the ice could have been 40 – 50 % consistent with Leppäranta et al. (2019). The internal deterioation is also a possible reason of the error about the ice rupture model. Yang et al. (2012) modelled ice breakup date turned out to be 12 d too late. The internal deterioration of the ice cover becomes extremely important, not only for the physics of ice, but also for spring ecology and the practical issues related to ice strength.

In spring, internal melting of ice can cause a significant reduction of the ice strength. This has two important consequences. First, the bearing capacity of ice decreases. The bearing capacity scales as $\sigma_f h^2$, where σ_f is the flexural strength. During the melting period, ice thickness decreases due to surface and bottom melting while ice strength decreases from internal melting. Due to the positive albedo feedback in the melting, the ice cover becomes patchy for its strength and the bearing capacity is largely unpredictable, that is a severe safety issue. Secondly, resistance of lake ice cover to breakage scales with $\sigma_c h/L$, where σ_c is compressive strength and L is the length scale of lake size. Decreasing thickness and strength may lead to breakage and ice movement on shores, where damage can be caused since the strength still is finite.

The deterioration of ice cover is not necessarily accompanied by an overall thinning of the ice cover. Since most engineering guidelines for bearing capacity are based on ice thickness and strength in relation to complete structural integrity, it is important to understand under what conditions these guidelines may be misleading. Therefore, it is necessary to know the ice porosity due to affections the level of force exerted on the structures. There are several models to relate porosity to failure stress (Ashton, 2012; Bulatov, 1970). Since boundary conditions of the crystals, and the density and porosity of ice need to be used in the model, the present study is of great help to the development of this kind of models.

The melting at both ice boundary and in ice interior was investigated in this study based on the field observation and calculation of heat budget. The results on the heat budget during the ice melt period can

https://doi.org/10.5194/tc-2022-232
Preprint. Discussion started: 5 December 2022

reveal the physical mechanisms behind seasonal formation and deteriorate of ice cover in different climatic conditions. The heat and mass transfer at the ice-water interface is the least studied among these mechanisms.The greater the heat flux from the water, the smaller ice thickness and the earlier the breakup time. For example, a heat flux of 1 W m^{-2} melts about 1 cm of ice every month, and the average melting rate of 1.3 cm d^{-1} ice breaks up about 1d earlier. The present study gave the heat flux corresponding to the bottom melting in two ice seasons, and the more transparent ice that allowed more sunlight penetration through ice in 2018 obtained larger heat flux than 2022. Compared with Lake Kilpisjärvi (Leppäranta et al., 2019), our fluxes were less than in a very warm year (15–20 W m^{-2}) but more than in a normal year (5–10 W m^{-2}). Much of the earlier literature has reported of smaller values at later stages of ice melting. Bengtsson et al. (1996) obtained for a number of small Swedish lakes the heat flux from water to ice ranging within 5−7 W m^{-2} in March−April. However, Jakkila et al. (2009) reported the heat flux values in Lake Pääjärvi as 12 W m^{-2} during the final stage of ice melting that is very close to the present results. Leppäranta et al. (2010) reported the heat flux of 7–29 W m^{-2} in late spring in the boreal Lake Vendyurskoye. The lake size may be the reason for the differences in water-ice heat fluxes, since in general the heat content is smaller and circulation weaker in small lakes. However, bottom melting remains the most uncertain component of the heat budget, and more field data and future research are needed particularly on the influence of the stage of ice melting, state of the under-ice boundary layer, and the amount of heat stored in the water during winter (Kirillin et al., 2018).

5.3 Ice melting impact on geochemistry

Deterioration of lake ice takes place at the top and bottom boundaries and in the interior. Porous melting ice is permeable to water, so that meltwater can flow down from top and lake water may penetrate to pores from below. These processes also influence the stratification of the surface water layer under the ice. The significance of meltwater to underwater chemistry and biology has not been much studied in lakes, apart from the density-driven stratification effect (Kirillin et al., 2012). Mathematical models for deterioration exist (Leppäranta, 2015) but are not in wide use, maybe because the melting period is short and once begun it progresses more or less steadily. Especially the gechemistry properties during ice melting period are rarely reported.

https://doi.org/10.5194/tc-2022-232
Preprint. Discussion started: 5 December 2022

Lake Pääjärvi was studied for ice and water geochemistry in mid-winter in 1996–1998 (Leppäranta et al., 2003). They measured the mean values of EC in snow, ice, and water as 16.5, 13 and 108 S cm^{-1} with the ranges of 4–28, 9.5–28 and 79–208 S cm^{-1}, respectively, and pH was 6.7 for ice and 6.6 for water. The value of pH in snow was typically 0.2 pH units lower than in ice. In this study, in 2022 the mean EC was in the snow-ice, congelation ice and lake water 13.0, 9.47 and 93.1 S cm^{-1} with the ranges of 7.53–31.1, 6.93–16.4 and 74.2–102.9 S cm^{-1}, respectively. It is worthy to notice that both pH and EC in ice melting period decreased with the ice decay and were smaller than in the mid-winter. After the melting started, the light under the ice increases due to the changes in the ice structure. The increase photosynthesis enhances CO_2 consumption and the pH of the water should be at a relatively higher level. There are two reasons for the lower pH: first, meltwater in ice was injected into water; second, biological activities under the ice became active with the rising of water temperature, and there was a surge of phytoplankton under ice resulting in an increase of CO_2, which leads to a continuous decline in pH value. But after the slush layer appeared, both pH and EC in ice increased due to lake water flushing. Based on the data of the inflows from brooks into the study bay. The current was almost static by April 21, whereas the inflow corresponded to 17 % of the water volume of the bay April 21–25. This means the geochemistry of the lake water was also affected by the brooks. Figure 9 showed the pH and EC of the inflow brooks and the results revealed the consistent changes with the lake.

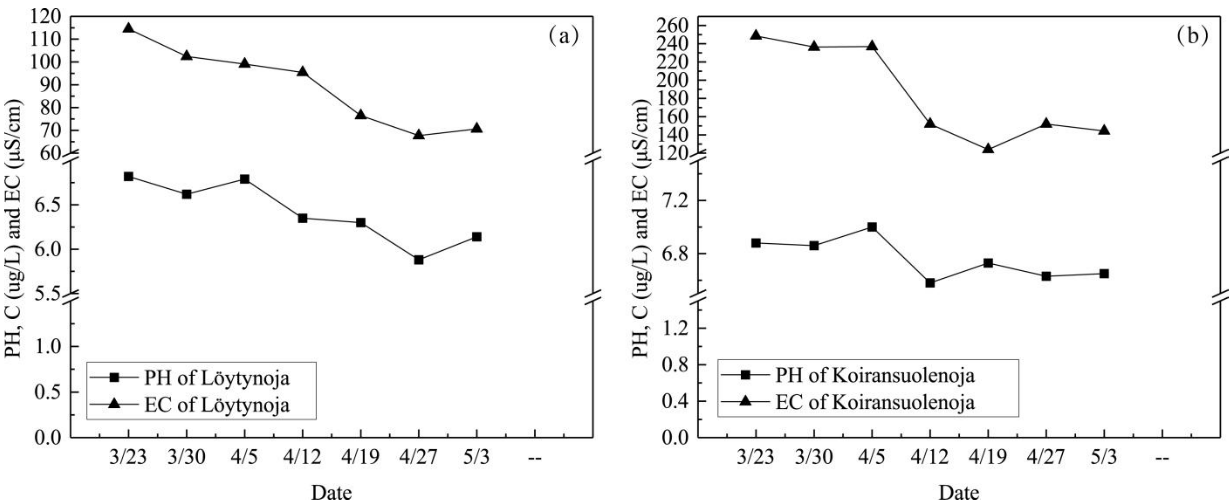

Figure 9. The pH and EC in Löytynoja (left) and Koiransuolenoja (right).

https://doi.org/10.5194/tc-2022-232
Preprint. Discussion started: 5 December 2022

The mean EC in ice was of the same order of magnitude but one order of magnitude lower than the lake water EC in both studies. The pH in snow-ice and congelation ice is a little lower than that in lake water in 2022 (Fig. 5). Flooding of lake water on ice and atmospheric deposition mostly imported the impurities into the ice cover. Snow-ice was formed of the snowfall with the melt-freeze cycles, flooding of the ice or liquid precipitation. Therefore, the deposition of acidic substances in the atmosphere was an important reason for the lower pH of snow-ice. The same result was found in 2018. The chl *a* is an indicator of phytoplankton biomass which can directly and quickly reveal the enrichment status of phytoplankton (Gradinger, 2002; Tedesco et al., 2012). Chl *a* was less than 0.5 g L^{-1} in ice and was lower than in the lake water. During the last two weeks of ice decay, water Chl *a* varied between 0.2 and 1.7 g L^{-1} which is of the same order of magnitude reported by previous research (Leppäranta et al., 2003; Vehmaa et al., 2009). The mean Chl *a* in ice was less than 0.5 g L^{-1}, 0.35 times of the lake water Chl *a*. Leppäranta et al. (2003) also reported the ratio of the Chl *a* in ice and water was 0.16. pH, EC and chl *a* are important indicators of water environmental quality. These environmental factors are not only the physical parameters of water environment, but also affect the physiological state of aquatic organisms, which will guide and predict the changes of biological structure in the water during the melting season.

6 Conclusions

The formation and decay of ice cover are changing under the influence of global warming. Due to the increasing attention to the climate impact on mid and high latitude lakes, more and more studies have been conducted on lake ice. Since it is very difficult to do fieldwork during the melting period, there are only few field data over the full ice decay period. The present has filled to this gap of knowledge focusing on the ice decay in Lake Pääjärvi, a boreal lake in southern Finland, in 2018 and 2022.

Lake ice melting and breakup form a fast, nonlinear process. The process is difficult to study in the field due to safety issues, and therefore relatively little is known about its details. The field observations were made in Lake Pääjärvi during the ice decay periods in 2018 and 2022. Ice monitoring was based on foot, hydrocopter, and boat, and a full time-series was obtained of the evolution of ice thickness, porosity, structure and geochemical properties through the melting period.

The results show how melting of lake ice takes place at the surface and bottom and in the interior simultaneously, and as a result ice thickness decreases and ice porosity increases. This drastically changes the physical properties of ice with consequences to the physics, chemistry, and biology of the waster body. The mechanical strength of ice decreases that has consequences to the bearing capacity of ice and ice forces. Also, weakened lake ice may be broken and pushed onshore by winds that causes shore area erosion and forces on man-made structures such as piers and navigation marks. The results are important for further development of numerical models towards more realistic physical presentation of the ice thickness and porosity during the decay period. This is well supported by the consistency between the field data of ice structure and thickness and the heat budget.

Data availability. The routine meteorological and hydrological data are available at: https://www.syke.fi and https://www.fmi.fi. The ice samples data applied in this work can be accessed by the link: https://doi.org/10.5281/zenodo.7342770.

Author contributions. YZ conceived the study with ML and wrote the paper. YZ performed the field work and lab work with contributions from LM, MF, JL, SS, and JA. All co-authors discussed the results and edited the manuscript.

Acknowledgements. We are grateful to the Lammi Biological Station and Institute of Atmospheric and Earth Sciences (University of Helsinki) for providing help with sample collection and processing. Thanks to Esa-Pekka Tuominen, Joni Uusitalo and Riitta IIola for helping the fieldwork and laboratory work. Thanks to Lauri Arvola for helping to edit the manuscript. This work was financially supported by the National Key Research and Development Program of China (Grant No. 2019YFE0197600), the National Natural Science Foundation of China (Grant No. 52211530038) and the Academy of Finland (350576), Personal grant to Yaodan Zhang by China Scholarship Council (CSC).

Competing interests. The authors declare that they have no conflict of interest.

References

Arst, H., Erm, A., Herlevi, A., Kutser, T., Leppäranta, M., Reinart, A., and Virta, J.: Optical properties of boreal lake waters in Finland and Estonia, Boreal Environ. Res., 13, 133–158, 2008.

Arvola, L., Kankaala, P., Tulonen, T., and Ojala, A.: Effects of phosphorus and allochthonous humic matter enrichment on metabolic processes and community structure of plankton in a boreal lake (Lake Pääjärvi), Can. J. Fish. Aquat. Sci., 53, 1646–1662, https://doi.org/10.1139/f96-083, 1996.

Arvola, L., Salonen, K., Keskitalo, J., Tulonen, T., Järvinen, M., and Huotari, J. : Plankton metabolism and sedimentation in a small boreal lake—a long-term perspective. Boreal Environ. Res., 19, 83-96, 2014.

Ashton, G. D.: Deterioration of Floating Ice Covers, J. Energy Resour. Technol.-Trans. ASME, 107, 177–182, https://doi.org/10.1115/1.3231173, 1985.

Ashton, G. D. (Eds.): River and lake ice engineering, Water Resources Publications, Littleton Colorado, 1986.

Benson, B. J., Magnuson, J. J., Jensen, O. P., Card, V. M., Hodgkins, G., Korhonen, J., Livingstone, D. M., Stewart, K. M., Weyhenmeyer, G. A., and Granin N. G.: Extreme events, trends, and variability in Northern Hemisphere lake-ice phenology (1855–2005), Climate Change, 112, 299–323, https://doi.org/10.1007/s10584-011-0212-8, 2012.

Bernhardt, J., Engelhardt, C., Kirillin, G., and Matschullat, J.: Lake ice phenology in Berlin–Brandenburg from 1947–2007: observations and model hindcasts, Climatic Change, 112, 791-817, https://doi.org/10.1007/s10584-011-0248-9, 2012.

Bengtsson, L., and Svensson, T.: Thermal Regime of Ice Covered Swedish Lakes, Hydrology Research, 27, 39–56, 1996.

Cavaliere, E., Baulch, H. M.: Denitrification under lake ice, Biogeochemistry, 137, 285–295,https://doi.org/10.1007/s10533-018-0419-0, 2018.

Garcia, S. L., Szekely, A. J., Bergvall, C., Schattenhofer, M., and Peura, S.: Decreased snow cover stimulates under-ice primary producers but impairs methanotrophic capacity. mSphere, 4, https://doi.org/10.1128/mSphere.00626-18, 2019.

Chow, R., Mettin, R., Lindinger, B., Kurz, T., and Lauterborn, W.: The importance of acoustic cavitation in the sonocrystallisation of ice-high speed observations of a single acoustic bubble, IEEE International Ultrasonics Symposium, Honolulu HI, USA, 5-8 October 2003, 1447-1450, https://doi.org/10.1109/ULTSYM.2003.1293177, 2003.

Deng, Y., Li, Z. K., Li, Z. J., and Wang, J.: The experiment of fracture mechanics characteristics of Yellow River ice, Cold Reg. Sci. Tech., 168, https://doi.org/10.1016/j.coldregions.2019.102896, 2019.

Ellis, A. W. and Johnson, J. J.: Hydroclimatic analysis of snowfall trends associated with the North American Great Lakes, J. Hydrol., 5, 471–486, https://doi.org/10.1175/1525-7541(2004)005<0471:HAOSTA>2.0.CO;2, 2004.

George, G. D.: The impact of the North Atlantic Oscillation on the development of ice on Lake Windermere, Climatic Change 81, 455–468, https://doi.org/10.1007/s10584-006-9115-5, 2007.

Grandineger, R.: Sea-ice algae: major contributors to primary production and algal biomass in the Chukchi and Beaufort Seas during May/June 2002, Deep-Sea Res. PT II., 56, 1201-1212, https://doi.org/10.1016/j.dsr2.2008.10.016, 2009.

https://doi.org/10.5194/tc-2022-232
Preprint. Discussion started: 5 December 2022

Griffiths, K., Michelutti, N., Sugar, M., Douglas, M. S. V., and Smol, J. P.: Ice-cover is the principal driver of ecological change in high Arctic lakes and ponds, PLoS One, 12, https://doi.org/10.1371/journal.pone.0172989, 2017.

Hampton, S. E., and Galloway, A. W. E., et al.: Ecology under lake ice, Ecol. Lett., 20, 98–111, https://doi.org/10.1111/ele.12699, 2017.

Iliescu, D., and Baker, I.: The structure and mechanical properties of river and lake ice, Cold Reg. Sci. Tech., 48, 202–217, https://doi.org/10.1016/j.coldregions.2006.11.002, 2007.

Jakkila, J., Leppäranta, M., Kawamura, T., Shirasawa, K., and Salonen K.: Radiation transfer and heat budget during the melting season in Lake Pääjärvi, Aquat. Ecol., 43, 681–692, https://doi.org/10.1007/s10452-009-9275-2, 2009.

Kärkäs, E.: The ice season of Lake Pääjärvi, southern Finland, Geophysica, 36, 85–94, 2000.

Karetnikov, S., Leppäranta, M., and Montonen, A.: Time series over 100 years of the ice season in Lake Ladoga, J. Gt. Lakes Res., 43, 979–988, https://doi.org/10.1016/j.jglr.2017.08.010, 2017.

Kirillin, G., Aslamov, I., Leppäranta, M., and Lindgren, E.: Turbulent mixing and heat fluxes under lake ice: the role of seiche oscillations, Hydrol. Earth Syst. Sci., 22, 6493-6504, https://doi.org/10.5194/hess-22-6493-2018, 2018.

Kirillin, G., Leppäranta, M., Terzhevik, A., Granin, N., Bernhardt, J., Engelhardt, C., Efremova, T., Golosov, S., Palshin, N., Sherstyankin, P., Zdorovennova, G., and Zdorovennov, R.: Physics of seasonally ice-covered lakes: a review, Aquat. Sci., 74, 659–682, https://doi.org/10.1007/s00027-012-0279-y, 2012.

Korhonen, J.: Long-term changes in lake ice cover in Finland, Hydrol. Res., 37, 347–363, https://doi.org/10.2166/nh.2006.019, 2006.

Kuusisto, E.: The thickness and volume of lake ice in Finland in 1961-90, Water and Environment Research Institute, 17, 27–36, 1994.

Langway, C. C.: Ice fabrics and the universal stage, Department of Defense, Department of the Army, Corps of Engineers, Snow Ice and Permafrost Research Establishmen, 1959.

Lei, R., Leppäranta, M., Erm, A., Jaatinen, E., and Pärn, O.: Field investigations of apparent optical properties of ice cover in Finnish and Estonian lakes in winter 2009, Est. J. Earth Sci., 60, 50–64, https://doi.org/10.3176/earth.2011.1.05, 2011.

Leppäranta, M., and Kosloff, P.: The thickness and structure of Lake Pääjärvi ice, Geophysica, 36, 233–248, 2000.

Leppäranta, M., Tikkanen, M., and Virkanen J.: Observations of ice impurities in some Finnish lakes, Proc. Estonian Acad Sci. Chem., 52, 59–75, 2003.

Leppäranta, M, Terzhevik, A., Shirasawa, K.: Solar radiation and ice melting in Lake Vendyurskoe, Russian Karelia, Hydrol. Res., 41, 50-62, https://doi.org/10.2166/nh.2010.122, 2010.

Leppäranta, M.: Interpretation of statistics of lake ice time series for climate variability, Hydrol. Res., 45, 673–683, https://doi.org/10.2166/nh.2013.246, 2014.

Leppäranta, M.: Freezing of lakes and the evolution of their ice cover, Springer, Berlin-Heidelberg, https://doi.org/10.1007/978-3-642-29081-7, 2015.

Leppäranta, M., Lindgren, E., Wen, L. J., and Kirillin, G.: Ice cover decay and heat balance in Lake Kilpisjärvi in Arctic tundra, J. Limnol., 78, 163–175, https://doi.org/10.4081/jlimnol.2019.1879, 2019.

Leppäranta, M., and Wen, L. J.,: Ice phenology in Eurasian lakes over spatial location and altitude, Water, 14, https://doi.org/10.3390/w14071037, 2022.

Li, Z. J., Jia, Q., Zhang, B. S., Leppäranta, M., Lu, P., Huang, W. F.: Influences of gas bubble and ice density on ice thickness measurement by GPR, Appl. Geophys., 7, 105–113, https://doi.org/10.1007/s11770-010-0234-4, 2010.

Masterson D. M.: State of the art of ice bearing capacity and ice construction, Cold Reg. Sci. Tech., 58:99-112, https://doi.org/10.1016/j.coldregions.2009.04.002, 2009.

Makkonen, L., and Tikanmäki, M.: Modelling frazil and anchor ice on submerged objects. Cold Reg. Sci. Tech., 151, 64–74, https://doi.org/10.1016/j.coldregions.2018.03.001, 2018.

Magnuson, J., Robertson, D., Benson, B., Wynne, R., Livingstone, D., Arai, T., Assel, R., Barry, R., Card, V., Kuusisto, E., Granin, N., Prowse, T., Stewart, K., and Vuglinski, V.: Historical trends in lake and river ice cover in the Northern Hemisphere, Science, 289, 1743–1746, https://doi.org/10.1126/science.289.5485.1743, 2000.

Rouse, W. R., Binyamin, J., Blanken, P. D., Bussières, N., Duguay C. R., Oswald, C. J., Schertzer, W. M., and Spence, C.: The influence of lakes on the regional energy and water balance of the central Mackenzie River Basin, In: Cold Region Atmospheric and Hydrologic Studies: The Mackenzie GEWEX Experience, edited by Woo, M. K., Springer, Berlin, 309–325, 2008a.

Rouse, W. R., Blanken, P. D., Duguay, C. R., Oswald, C. J. and Schertzer, W. M. : Climatelake interations. In: Cold Region Atmospheric and Hydrologic Studies: The Mackenzie GEWEX Experience, edited by Woo, M. K., Springer, Berlin, 139–160, 2008b.

SFS 3008. Determination of total residue and total fixed residue in water, sludge and sediment. Suomen standardisoimisliitto SFS, 1990.

SFS-EN 27888. Water quality. Determination of electrical conductivity. Suomen standardisoimisliitto SFS, 1994.

Shumskii, P.A.: Principles of structural glaciology, Translated from the Russian by Kraus, D., Dover Publications, New York, 497pp, 1956.

Sharma, S.; Blagrave, K.; Magnuson, J. J.; O'Reilly, C. M.; Oliver, S.; Batt, R. D.; Magee, M. R.; Straile, D.; Weyhenmeyer, G. A.; and Winslow, L.: Widespread loss of lake ice around the Northern Hemisphere in a warming world, Nat. Clim. Chang., 9, 227–231, https://doi.org/10.1038/s41558-018-0393-5, 2019.

Schroth, A. W., Giles, C. D., Isles, P. D. F., Xu, Y. Y., Perzan, Z., and Druschel, G. K.: Dynamic coupling of iron, manganese, and phosphorus behavior in water and sediment of shallow ice-covered eutrophic lakes, Environ. Sci. Technol., 49, 9758–9767, https://doi.org/10.1021/acs.est.5b02057, 2015.

Shirasawa, K., Leppäranta, M., Kawamura, T., Ishikawa, M., and Takatsuka, T.: Measurements and modelling of the water-ice heat flux in natural waters, Proceedings of the 18th IAHR International Symposium on Ice, Hokkaido University, Sapporo, Japan, 28 August–September 2006, 85–91, 2006.

https://doi.org/10.5194/tc-2022-232
Preprint. Discussion started: 5 December 2022

Shoshany, Y., Prialnik, D., Podolak, M.: Monte Carlo modeling of the thermal conductivity of porous cometary ice. Icarus, 157, 219–227, https://doi.org/10.1006/icar.2002.6815, 2002.

Stefan, H. G., and Fang, X.: Simulated climate change effects on ice and snow covers on lakes in a temperate region, Cold Reg. Sci. Tech., 25, 137–152, https://doi.org/10.1016/S0165-232X(96)00023-7, 1997.

Timco, G. W., and Frederking R. M. W.: A review of sea ice density, Cold Reg. Sci. Tech., 24, 1−6, https://doi.org/10.1016/0165-232X(95)00007-X, 1996.

Tedesco, L., Vichi, M., and Thomas, D. N.: Process studies on the ecological coupling between sea ice algae and phytoplankton, Ecol. Model., 226, 120-138, https://doi.org/10.1016/j.ecolmodel.2011.11.011, 2012.

Tan, Z., Yao, H. X., and Zhuang, Q. L.: A small temperate lake in the 21st century: Dynamics of water temperature, ice phenology, dissolved oxygen, and chlorophyll a, Water Resour. Res., 54, 4681–4699, https://doi.org/10.1029/2017WR022334, 2018.

Vehmaa, A., and Salonen, K.: Development of phytoplankton in Lake Pääjärvi (Finland) during under-ice convective mixing period, Aquat. Ecol., 43, 693–705, https://doi.org/10.1007/s10452-009-9273-4, 2009.

Warren, S.,G.: Optical properties of snow, Rev. Geophys., 20, 67–89, https://doi.org/10.1029/RG020i001p00067, 1982.

Williams, G., Layman, K. L. and Stefan, H. G.: Dependence of lake ice covers on climatic, geographic and bathymetric variables, Cold Reg. Sci. Tech., 40, 145–164, https://doi.org/10.1016/j.coldregions.2004.06.010, 2004.

Wang, C. X., Shirasawa, K., Leppäranta, M., Ishikawa, M., Huttunen, O., and Takatsuka T.: Solar radiation and ice heat budget during winter 2002–2003 in Lake Pääjärvi, Finland, Verh. Internat. Verein Limnol., 29, 414–417, https://doi.org/10.1080/03680770.2005.11902045, 2005.

Yang, Y., Leppäranta, M., Cheng, B., and Li, Z. J.: Numerical modelling of snow and ice thicknesses in Lake Vanajavesi, Finland, Tellus Ser. A-Dyn. Meteorol. Oceanol., 64, https://doi.org/10.3402/tellusa.v64i0.17202, 2012.